Dispersion properties of nonradiating configurations: Finite-difference time-domain modeling

A. D. Boardman and K. Marinov*

Photonics and Nonlinear Science Group, Joule Laboratory, Department of Physics, University of Salford, Salford M5 4WT, United Kingdom

N. Zheludev† and V. A. Fedotov

EPSRC Nanophotonics Portfolio Centre, School of Physics and Astronomy, University of Southampton, Highfield, Southampton, SO17 1BJ, United Kingdom

A finite-difference time-domain (FDTD) numerical analysis is used to demonstrate that a toroidal solenoid, coaxial with an electric dipole, is a remarkable nonradiating configuration. It can be used to measure the dielectric permittivity of any ambient matter. It becomes a directional radiator at an interface between two dielectric media, depositing energy in the material with the highest polarizability.

PACS number(s): 41.20.Jb, 42.25.Gy

I. INTRODUCTION

Toroidal and supertoroidal structures are widely present in nature and a supertoroid was explicitly drawn by Leonardo in 1490. The simplest examples of such objects would be toroidal solenoids with currents in them. More generally, fractal complications of the simple toroidal wiring known as supertoroidal structures are discussed and toroidal arrangements of electric and magnetic dipoles have been discussed in the literature. Today the main biological journals feature an increasing number of papers on proteins, viruses and phages possessing elements of toroidal and supertoroidal symmetry. At the same time we witness a growing stream of theoretical papers on the electrodynamics and optics of toroidal and supertoroidal currents, toroidal nanostructures, toroidal microscopic moments and interactions of electromagnetic fields with toroidal configuration. Recent studies of phase transitions in ferroelectric nanodisks and nanorods [1] and toroidal arrangements of spins in magnetic structures [2] show growing interest in studying toroidal structures from the materials research community.

Here we report a rigorous finite-difference time-domain numerical analysis proving that a toroidal solenoid with poloidal wiring coaxial with an electric dipole is a remarkable nonradiating configuration. The property not to radiate electromagnetic energy is based on the destructive interference between the fields created by each of its constituents. We show that this configuration may be used as a sensor for the dielectric permittivity of the ambient matter. It becomes a directional radiator at an interface between two dielectric media depositing energy in the material with highest polarizability.

Nonradiating configurations are such oscillating charge-current distributions that do not produce electromagnetic fields in the radiation zone. An early work [3] shows that the orbital motion of a uniformly charged spherical shell of ra-dius R will not produce any radiation if the radius R of the shell is equal to $lcT/2$ where c is the speed of light, T is the period of the orbit, and l is an integer number. The general problem for absence of radiation from an arbitrary localized charge distribution, exhibiting periodic motion with period $T = 2\pi/\omega_0$, has been addressed [4] and it has been shown that such a system does not generate electromagnetic potentials in the radiation zone if the Fourier components $\tilde{J}(l\omega_0 \mathbf{r}/cr, l\omega_0)$ are not present in the spectrum of the current density $\mathbf{J}(\mathbf{r}, t)$. This criterion also explains the behavior of an orbiting uniformly charged sphere. It has been pointed out in [4] that this condition may not be necessary. It indeed ensures the disappearance of the electromagnetic potentials in the radiation zone; however, calculations of the power emitted by the system show that its value is zero provided that $\tilde{J}(l\omega_0 \mathbf{r}/cr, l\omega_0) \propto \mathbf{r}$, which is a weaker sufficient condition. Indeed, the latter condition only requires the absence of the components transverse to the wave vector. It has been proved rigorously [5] that the absence of the transverse components of the Fourier spectrum of the current density is a necessary and sufficient condition for absence of radiation. Interestingly, such a condition has appeared in an earlier study, [6], in connection with electromagnetic self-force action and self-oscillations of a nonrelativistic particle.

The important conclusion that can be drawn from the earlier results is that two types of nonradiating configurations can exist in principle. For the first type the Fourier components $\tilde{J}(\omega \mathbf{r}/cr, \omega)$ of the current density are zero. Numerous examples of systems pertaining to this sort of nonradiating configurations exist [3,4,7]. A characteristic feature of these systems is that *both* the electromagnetic fields and the electromagnetic potentials are zero. For the second type of nonradiating configurations the Fourier spectrum is purely longitudinal, i.e., $\tilde{J}(\omega \mathbf{r}/cr, \omega) \propto \mathbf{r}$. Here the electromagnetic fields are zero but as we show the electromagnetic potentials may be finite.

Interestingly, it is pointed out [4] that the case of $\tilde{J}(\omega \mathbf{r}/cr, \omega) \propto \mathbf{r}$ corresponds to trivial spherically symmetric radial oscillations of the charge density. Nevertheless non-

---

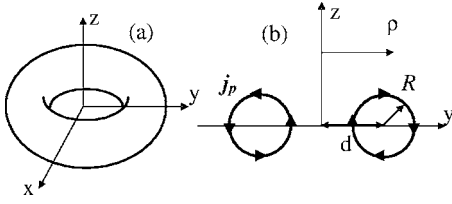*Electronic address: k.marinov@salford.ac.uk

†URL: http://www.nanophotonics.phys.soton.ac.uk

FIG. 1. Toroidal surface (a) and its cross section with the $z-y$ plane (b). The triangles show the direction of the surface current j_p.

trivial examples can be created using toroidal structures. Recent papers [7,8] show that a non-radiating configuration can be constructed by combining an infinitesimal toroidal solenoid with poloidal current flowing in its windings (i.e., along the meridians of the toroid) with an electric dipole placed in the center of the toroid. The explicit calculations of [7 and 8] show that while the electromagnetic fields disappear outside such a composite object, the electromagnetic potentials survive. As we show here this particular structure belongs to the second type of nonradiating systems and that it is the longitudinal part of the Fourier spectrum of the current density which is responsible for the residual electromagnetic potentials in the radiation zone.

The results of [7,8] suggest that the nonradiating configurations involving toroidal solenoids may have a number of interesting electromagnetic properties. These properties however have never been studied in proper detail. This is the aim of the present study.

The physical nature of the problem is extremely well suited to numerical modeling using the FDTD method [9] which will be used in our analysis. It gives the possibility to address the electromagnetic properties of this specific structure consisting of a toroid coupled to a dipole in full numerical detail. In addition, an assessment of what possible applications such structures might have is given.

Exact compensation between the fields generated by a toroidal solenoid and an electrical dipole takes place for infinitesimal objects only. It therefore seems plausible that assessment of the extent to which the properties of the infinitesimal nonradiating configurations are preserved by finite-dimensional counterparts should precede possible experimental designs. It is important also to determine what is the behavior of these structures under certain (nontrivial) perturbations.

II. INFINITESIMAL TOROIDAL SOLENOIDS AND NONRADIATING CONFIGURATIONS

The electromagnetic properties of toroidal solenoids and toroidal helix antennas are studied in detail in Refs. [10–16]. Here only the results that will be used in our exposition are briefly summarized.

The current flowing along the meridians of a toroidal solenoid (known also as poloidal current, Fig. 1) can be presented in the form (see, e.g. [14])

$$j_p = \nabla \times M, \qquad (1)$$

since $\nabla \cdot j_p = 0$. In Eq. (1) j_p is the current density vector and $M = (0, M_\varphi, 0)$ is the azimuthal magnetization vector, given by

$$M_\varphi = \frac{NI(t)}{2\pi\rho} \qquad (2)$$

if $(\rho - d)^2 + z^2 < R^2$ and zero otherwise. In Eq. (2) N is the total number of windings and $I[A]$ is the magnitude of the current. Pursuing this idea a step further the magnetization M can in turn be expressed as

$$M = \nabla \times T, \qquad (3)$$

where $T = (0, 0, T_z)$ is called toroidization vector. The general problem is difficult to perform analytically [10–13] and any limit that preserves the correct properties while at the same time giving valuable mathematical simplification is a step worth taking. Such a step is $d \to 0$. This is a useful step because it gives the toroidization vector in the following form (see, e.g. [7,14]):

$$T_z = \frac{\pi N I d R^2}{2} \delta^3(r). \qquad (4)$$

Assuming monochromatic time dependence, $\propto \exp(-i\omega t)$, and using (4) the magnetic field created by the toroidal solenoid can be obtained in the form

$$H_p = \frac{N I d R^2}{8} \frac{k^2}{r^2}\left(ik - \frac{1}{r}\right)(r \times n)\exp(ikr), \qquad (5)$$

where n is a vector of unit length pointing along the z axis and k is the wave vector.

A dipole can be introduced at the center of the toroid. If this dipole is modeled as a piece of wire of length L_d with the current strength being equal to I_d the dipole moment amplitude, p_0, can be expressed through $iL_dI_d = \omega p_0$, where $p_0 = p_0 n$. The magnetic field of the dipole is [17]

$$H_d = \frac{\omega k}{4\pi}\left(1 - \frac{1}{ikr}\right)(r \times p_0)\frac{\exp(ikr)}{r^2}. \qquad (6)$$

The time-averaged power P emitted by the composite object (an infinitesimal toroidal solenoid coupled to an electrical dipole) is given by

$$P = \frac{\mu_0 c k^2}{12\pi\sqrt{\epsilon}}(I_dL_d + k^2T)^2, \qquad (7)$$

where $T = \pi N I d R^2 / 2$ and ϵ is the relative dielectric permittivity of the ambient matter.

This expression can be generalized to include higher-order multipole moments [15].

Equation (7) can be rewritten in the form

$$P = \frac{\mu_0 c k^2 (I_dL_d)^2}{12\pi\sqrt{\epsilon}}\left(1 - \frac{\epsilon}{\tilde{\epsilon}}\right)^2, \qquad (8)$$

where

$$\tilde{\epsilon} = -\frac{I_dL_dc^2}{\omega^2 T} \qquad (9)$$

is the effective relative dielectric permittivity of the medium in which electromagnetic fields of the toroid and the electric dipole can compensate each other. This suggests that it

should be possible to measure the relative dielectric permittivities of media (e.g., liquids) by adjusting experimentally the ratio of the currents I_d and I until a minimum of the emitted power is detected. Then the relative dielectric constant of the material under investigation can be obtained from (9).

It has been pointed out in [8] that while the electromagnetic fields disappear when the compensation condition (9) is satisfied the electromagnetic potentials survive. However, there are examples of non-radiating configurations (see, e.g. [4,7]) for which *both* the electromagnetic fields and the electromagnetic potentials are zero. The question is then what is the physical reason for that and what is the difference between both types of electromagnetic systems. Following [4,5] it can be shown that the difference is in the current-density spectra. To see this consider the vector potential

$$A = \frac{\mu_0}{4\pi} \int \frac{j\left(r', t - \frac{|r - r'|}{c}\right)}{|r - r'|} d^3 r'. \tag{10}$$

In the radiation zone the standard approximation [17] can be used and (10) reduces to

$$A = \frac{\mu_0}{4\pi r} \int j(r', t - r/c + r \cdot r'/cr) d^3 r'. \tag{11}$$

Now if the current density $j(r, t)$ is expressed through its Fourier-transform

$$j(r, t) = \int \tilde{j}(k, \omega) e^{-i(\omega t - k \cdot r)} d^3 k \, d\omega, \tag{12}$$

Eq. (11) becomes

$$A = \frac{\mu_0 (2\pi)^3}{4\pi r} \int \tilde{j}\left(\frac{\omega r_0}{c}, \omega\right) e^{-i\omega(t - r/c)} d\omega, \tag{13}$$

where $r_0 = r/r$. As Eq. (13) shows only those components of the current density spectrum that correspond to $|k| = \omega/c$ contribute to radiation [5]. It is immediately clear that if the condition

$$\tilde{j}\left(\frac{\omega r_0}{c}, \omega\right) = 0 \tag{14}$$

is satisfied then the vector potential vanishes. Using the continuity equation, the Fourier-components of the charge density can be expressed from the Fourier-components of the current density according to $\rho(k, \omega) = k \cdot \tilde{j}(k, \omega)/\omega$ and by following a procedure similar to deriving Eq. (13) but this time for the scalar potential it can be shown that the scalar potential is also zero if (14) is satisfied. Therefore (14) ensures that the electromagnetic system considered is a nonradiating configuration. This general statement is a sufficient condition [4].

The results of [5] imply however that the condition (14) is *not* necessary. With the assumption of a monochromatic time dependence (13) reduces to

$$A = \frac{\mu_0 (2\pi)^3}{4\pi r} \tilde{j}\left(\frac{\omega r_0}{c}, \omega\right) e^{-i\omega(t - r/c)}. \tag{15}$$

The electromagnetic fields can then be obtained using $H = \nabla \times A/\mu_0$ and $E = i\nabla \times H/\omega \epsilon_0$. Beacause (15) is valid in the radiation zone only, r_0 and $1/r$ must be treated as constants in deriving the fields from the vector potential. The result is

$$E = i\sqrt{\frac{\mu_0}{\epsilon_0}} \frac{\omega (2\pi)^3}{4\pi c r} r_0 \times (\tilde{j} \times r_0) e^{-i\omega(t - r/c)} \tag{16}$$

and

$$H = i\frac{\omega (2\pi)^3}{4\pi c r} (r_0 \times \tilde{j}) e^{-i\omega(t - r/c)}. \tag{17}$$

From (16) and (17) it is clear that the time-averaged Poynting vector, $\langle S \rangle = (1/2) E \times H^*$, can be presented in the form

$$\langle S \rangle \propto |r_0 \times (\tilde{j} \times r_0)|^2 r_0. \tag{18}$$

The quantity $r_0 \times (\tilde{j} \times r_0)$ is the radiation pattern of the system. As can be seen from (18) a charge-current distribution will not emit electromagnetic energy if

$$\tilde{j}_\perp \equiv r_0 \times (\tilde{j} \times r_0) = 0 \tag{19}$$

which is a weaker sufficient condition compared to (14). The fact that (19) is also a necessary condition for the absence of radiation can be seen by setting E and H to zero in (16) and (17) and this was established in [5]. However (19) has appeared in the earlier studies [4,6].

The identity $\tilde{j} = r_0 \times (\tilde{j} \times r_0) + r_0 (r_0 \cdot \tilde{j}) = \tilde{j}_\perp + \tilde{j}_\parallel$ and the comparison of (19) with (14) show that systems satisfying (14) will emit no electromagnetic energy and will not produce electromagnetic potentials. On the other hand, for systems satisfying the weaker condition (19) the electromagnetic potentials are not necessarily zero, since the longitudinal (parallel to r_0) part of the current-density spectrum $\tilde{j}_\parallel$ will contribute to the vector potential according to Eq. (15).

It is easy to show that the nonradiating configuration consisting of a toroidal solenoid coaxial with an electric dipole is an example of the second type of nonradiating configurations—systems satisfying (19) and not (14). The current density associated with this system is $j(r) = T\nabla \times [\nabla \times n\, \delta^3(r)] + I_d L_d n\, \delta^3(r)$ and its Fourier spectrum is given by

$$(2\pi)^3 \tilde{j}(k) = -Tk(k \cdot n) + (k^2 T + I_d L_d) n. \tag{20}$$

For values of $k = \omega\sqrt{\epsilon} r_0/c$ and using the compensation condition (9), Eq. (20) reduces to

$$(2\pi)^3 \tilde{j}\left(\frac{\omega r_0}{c}\right) = -T\frac{\omega^2 \epsilon}{c^2} r_0 (r_0 \cdot n). \tag{21}$$

As (21) shows the current density spectrum is purely parallel to r_0 for wave number values $|k| = \omega\sqrt{\epsilon}/c$. It can be concluded that it is the survival of the longitudinal part of the current density spectrum that gives the possibility to create
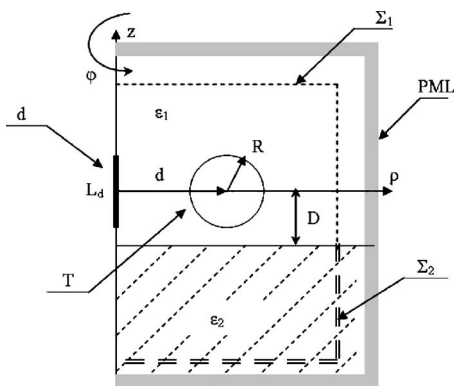
FIG. 2. Nonradiating configuration consisting of a toroidal solenoid and an electric dipole near the interface between two materials. Cylindrical symmetry is assumed. PML: perfectly matched layer; d: dipole; T: toroid; Σ_1, Σ_2: cylindrical surfaces used to calculate the power emitted in each of the materials with $\epsilon = \epsilon_1$ and $\epsilon = \epsilon_2$, respectively.

nonzero electromagnetic potentials in the radiation zone in the absence of electromagnetic fields.

III. NUMERICAL MODELING OF THE INTERACTION OF A NON-RADIATING CONFIGURATION WITH THE INTERFACE BETWEEN TWO MATERIALS

As can be seen from Sec. II the composite emitter—toroid and dipole—becomes a nonradiating configuration [note that the compensation condition (9) is satisfied] due to the destructive interference between the electromagnetic fields created by the toroid and by the electric dipole. This interference occurs in all possible directions in a homogeneous medium. In an *inhomogeneous* material however as would be encountered for an interface between two dielectrics with relative permittivity constants ϵ_1, and ϵ_2 this does not happen. To appreciate this consider the situation shown in Fig. 2, in which an emitter consisting of an electric dipole and a toroidal solenoid is placed in a medium with dielectric permittivity equal to ϵ_1. This medium is separated from a second one by a planar interface located at a distance D from the equatorial plane of the toroid. In the absence of the interface the system is nonradiative and the effective permittivity is $\tilde{\epsilon} = \epsilon_1$. In order to assess the consequences flowing from the presence of the interface between the two dielectrics and also the finite size of both the toroid and the dipole it is necessary to solve the Maxwell's equation exactly. This can be achieved numerically using the FDTD method [9]. The latter can be considerably simplified since the toroid is a body of revolution (BOR). Taking advantage of the axial symmetry reduces the problem to a two-dimensional one. Cylindrical coordinates can be used and there is no dependence on the azimuthal variable angle φ (Fig. 2). This implementation of the FDTD method is known as BOR-FDTD [9]. The computational domain is terminated by a standard perfectly matched layer (PML) [9,18]. The radiation of both the toroid and the dipole is categorized by the field components (E_ρ, E_z, H_φ) that are not identically zero and hence it is of E-type (TM) [14]. The applicability of the FDTD method to
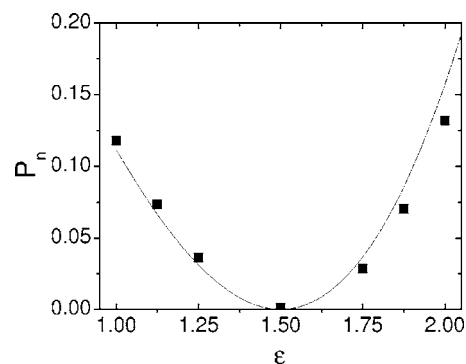

FIG. 3. Normalized emitted power $P_n = 12 P \pi c / [\mu_0 (I_d L_d \omega)^2]$ versus the relative dielectric permittivity ϵ of the ambient dielectric material. The value of $\tilde{\epsilon}$ [Eq. (9)] is $\tilde{\epsilon} = 1.5$. The solid curve and the solid squares are the analytical result [Eq. (8)] and the numerical result, respectively.

radiating structures (antenna problems) is well established and this technique has been successfully applied to various designs [19–21]. In the model the poloidal current j_p, is expressed through the azimuthal component of the magnetization which is consistent with the assumption that all the parts of the toroid respond simultaneously (or with negligible delay) to the driving voltage. This is expected to occur when the size of the toroid is much smaller than the wavelength. To evaluate the directional properties of the emitting structure studied, the quantities P_1 and P_2 are introduced and defined as

$$P_i = \int_{\Sigma_i} \langle S \rangle \cdot d\Sigma_i, \quad i = 1, 2. \tag{22}$$

In (22) $\langle S \rangle$ is the time-averaged Poynting vector and Σ_1, Σ_2 (see Fig. 2) are cylindrical surfaces placed away from the source (close to the PML region) in order to ensure that the near-field contributions have negligible effect on the power values calculated according to (22).

IV. RESULTS AND DISCUSSION

In order to model the behavior of the nonradiating configuration the following parameter values are selected. The larger and the smaller radii of the toroidal solenoid are fixed to $d = 1$ cm and $R = 0.5$ cm, respectively, the dipole length is $L_d = 0.9$ cm and the excitation frequency is $\omega / 2\pi = 1$ GHz. The FDTD-grid resolution is $\Delta\rho = \Delta z = \lambda / 300$, where λ is the free-space wavelength. Since Eq. (8) is strictly valid for infinitesimal objects only, it is necessary to make sure that for the selected values of the parameters the contributions from the higher-order multipoles are negligible. To verify this Eq. (8) has been compared with results obtained from FDTD simulations in a homogeneous material (this pertains to the case of $\epsilon_1 = \epsilon_2 = \epsilon$ in Fig. 2) and the result is presented in Fig. 3. The simulations are in good agreement with Eq. (8). This means that for the selected values of the parameters the contributions of the toroidal dipole moment and the electrical dipole moment are dominant.

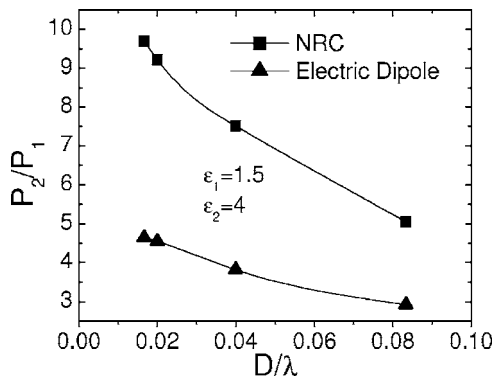Figure 4 compares the directional properties of a *per-*

FIG. 4. The ratio between the powers P_1 and P_2 emitted in the materials with dielectric constant ϵ_1 and ϵ_2, respectively, by a nonradiating configuration (NRC, solid squares) and an electric dipole (electric dipole, solid triangles) as a function of the distance D between the emitter and the interface. The parameter $\tilde{\epsilon}$ of the nonradiating configuration is $\tilde{\epsilon} = \epsilon_1$.

turbed nonradiating configuration with that of an electric dipole. The ratio between the power values P_1 and P_2 emitted in the materials with dielectric constants ϵ_1 and ϵ_2, is computed for several values of the distance D using either a nonradiating configuration or an electric dipole. The presence of the interface affects both types of emitters. However, Fig. 4 shows that a larger fraction of the total emitted power can be directed in the material with $\epsilon = \epsilon_2$ for the case in which the emitter is a nonradiating configuration. Comparing the performance of the nonradiating configuration with that of the dipole acting along shows that the nonradiating configurations has a clear advantage in the ability to direct a larger fraction of the total emitted power in a material with higher value of the dielectric constant. This advantage disappears in the proportion of the increase of the distance to the interface. It has been verified that the dependence of the ratio P_2/P_1 on the distance D for both the emitters stems mainly from the dependence of the quantity P_2 on D. The value of P_1 appears to be less susceptible to the variations of D for this range of parameter values. For some applications it might be desirable to direct electromagnetic energy within a certain material while little or no energy is emitted to the surrounding space. It seems that a non-radiating configuration with $\tilde{\epsilon} = \epsilon_1$ may be suitable for this purpose. Relatively far from the interface it does not radiate at all, or radiates a small amount of power. Bringing the nonradiating configuration into contact with the interface will lead to an increase of the total emitted power $P_1 + P_2$, (keeping the values of the currents I_d and I fixed) with the contribution P_2 predominating strongly.

To study this property further, Fig. 5 and Fig. 6 show the dependence of the ratio P_2/P_1 on the dielectric constant of the substrate for two fixed values of the distance D between the emitters and the interface and $\tilde{\epsilon} = \epsilon_1$. The directional properties of the non-radiating composite object are compared with those of its constituents—the electrical dipole and the toroidal solenoid. As Fig. 5 and Fig. 6 show, the ratio P_2/P_1 for the toroidal solenoid and for the electrical dipole shows little dependence on the dielectric constant of the substrate ϵ_2. At same time, when nonradiating configuration is used as
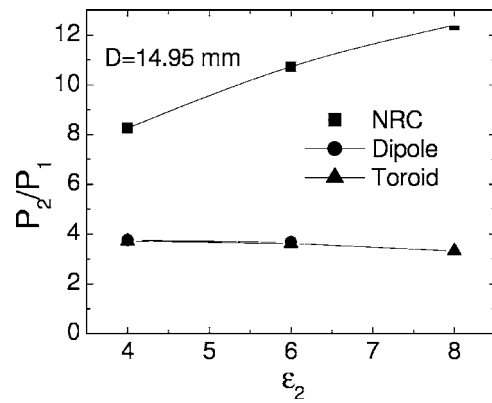

FIG. 5. The ratio between the powers P_1 and P_2 emitted in the materials with dielectric constant ϵ_1 and ϵ_2, respectively, by a nonradiating configuration (NRC, solid squares), electrical dipole (dipole, solid circles) and the toroidal solenoid (toroid, solid triangles) as a function of the dielectric constant ϵ_2. The parameter $\tilde{\epsilon}$ of the nonradiating configuration is $\tilde{\epsilon} = \epsilon = 1$ and the distance between the emitters and the interface is $D = 14.95$ mm.

an emitter, not only the ratio P_2/P_1 is higher, but it increases strongly with the increase of ϵ_2. This shows that in the region of parameter values studied the directional properties of the nonradiating configuration improve with the increase of the contrast between the relative dielectric permittivities of the two materials. A comparison between Fig. 5 and Fig. 6 shows that as the nonradiating configuration approaches the interface its performance improves. Indeed, it can be concluded that the optimum performance is achieved when the nonradiating configuration is in direct contact with the interface. This feature is in agreement with Fig. 4. The dependence of the emission properties of the nonradiating configuration upon the values of the dielectric constant of the substrate is suitable for sensor applications.

The results presented in Fig. 6 are visually presented in Fig. 7 and Fig. 8 where the spatial distribution of the time-averaged Poynting vector around two of the studied emitters—nonradiating configuration and a toroidal solenoid—is shown. The Poynting vector values are normalized to the value of the total emitted power to allow a comparison at identical total emitted powers to be made. As can be seen the electromagnetic field created by the nonradiating
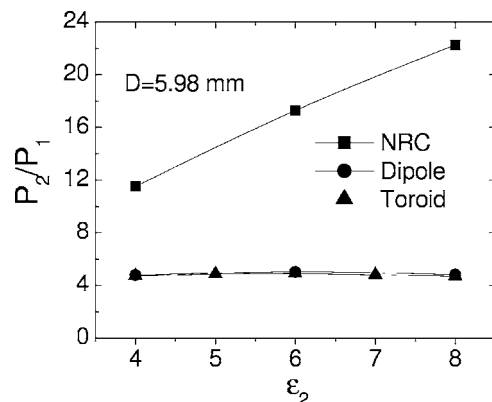

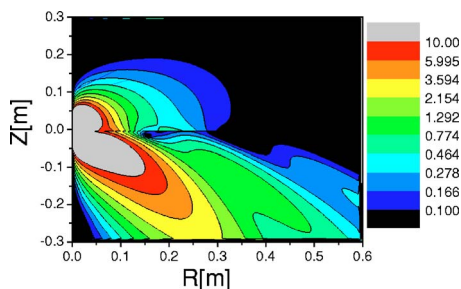FIG. 6. The same as in Fig. 5 but for $D = 5.98$ mm.

FIG. 7. (Color online) Spatial distribution of the time-averaged and normalized Poynting vector modulus $\langle\sqrt{S_\rho^2 + S_z^2}\rangle/(P_1 + P_2)$ for a nonradiating configuration. The distance between the emitter and the interface is $D = 5.98$ mm. Note that logarithmic scale is used for the values of the Poynting vector. The values of the other parameters are $\tilde{\epsilon} = \epsilon_1 = 1$ and $\epsilon_2 = 8$.

FIG. 8. (Color online) The same as in Fig. 7 but the emitter here is a toroid.

configuration in free space ($\epsilon = 1$) is weak compared to that emitted by the toroidal solenoid. This shows that a larger fraction of the total emitted power is deposited in the substrate material.

V. CONCLUSIONS

In conclusion, we studied a remarkable nonradiating configuration consisting of a toroidal solenoid coupled to an electri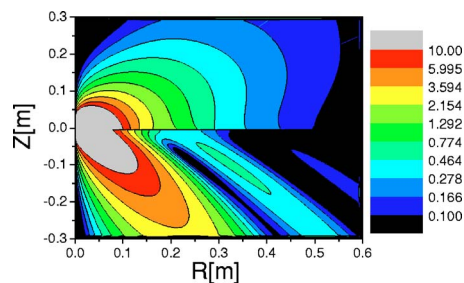cal dipole. The property not to radiate electromagnetic energy is based on the destructive interference between the fields created by each of its constituents. We show that the interference effect depends on the dielectric characteristics of the ambient matter and the configuration may be used in dielectric permittivity measurements. It becomes a directional radiator at an interface between two dielectric media depositing energy in the material with the highest polarizability.

[1] I. I. Naumov, L. Bellaiche, and H. Fu, Nature (London) **432**, 737 (2004).

[2] K. Klaui, C. A. F. Vaz, L. Lopez-Diaz, and J. A. C. Bland, J. Phys.: Condens. Matter **15**, R985 (2003).

[3] G. A. Schott, Philos. Mag. **15**, (7) 752 (1933).

[4] G. H. Goedecke, Phys. Rev. **135**, B281 (1964).

[5] A. J. Devaney and E. Wolf, Phys. Rev. D **8**, 1044 (1973).

[6] D. Bohm and M. Weinstein, Phys. Rev. **74**, 1789 (1948).

[7] G. N. Afanasiev and V. M. Dubovik, Phys. Part. Nucl. **29**, 366 (1998).

[8] G. N. Afanasiev and Yu. P. Stepanovsky, J. Phys. A **28**, 4565 (1995).

[9] A. Taflove and S. Hagness, *Computational Electrodynamics: The Finite-Difference Time-Domain Method* (Artech House, Norwood, MA, 2000).

[10] G. N. Afanasiev, J. Phys. A **26**, 731 (1993).

[11] G. N. Afanasiev, J. Phys. A **23**, 5755 (1990).

[12] G. N. Afanasiev and V. M. Dubovik J. Phys. A **25**, 4869 (1992).

[13] G. N. Afanasiev, V. M. Dubovik, and S. Misicu J. Phys. A **26**, 3279 (1993).

[14] G. N. Afanasiev, J. Phys. A **34**, 539 (2001).

[15] V. M. Dubovik and V. V. Tugushev, Phys. Rep. **187**, 145 (1990).

[16] L. W. Li, P. N. Jiao, X. W Shi, and J. A Kong, IEEE Trans. Antennas Propag. **52**, 2381 (2004).

[17] J. D. Jackson, *Classical Electrodynamics* (Wiley, New York, 1999).

[18] F. L. Teixeira and W. C. Chew, IEEE Microw. Guid. Wave Lett. **7**, 285 (1997).

[19] J. G. Maloney, G. S. Smith, and W. R. Scott, IEEE Trans. Antennas Propag. **38**, 1059 (1990).

[20] J. G. Maloney and G. S. Smith, IEEE Trans. Antennas Propag. **41**, 668 (1993).

[21] P. Tirkas and C. Balanis, IEEE Trans. Antennas Propag. **40**, 334 (1992).